A Radial Folding Mechanism to Enable Surgical Continuum Manipulators to Fit Through Smaller Ports

Mariana E. Smith*[1], Daniel S. Esser*[1], Margaret Rox[1], Alan Kuntz[2], and Robert J. Webster III[1]

***Abstract*— Tendon driven continuum robots promise tentacle-like dexterity in minimally invasive surgical applications. These robots are subject to conflicting design goals. It is desirable for the robot to fit through the smallest port possible, yet it is also desirable for the robot's diameter to be large, so that for a given tension, tendons can apply larger actuation moments to the robot. To satisfy both goals simultaneously, we propose a new radial folding mechanism that facilitates a 2.5x diameter change along the robot. We show that our folding tendon manipulator can be modeled by existing mechanics-based models. Comparing at consistent tendon tensions, the robot has a larger range of motion and larger stiffness than a non-folding continuum robot that fits through the same sized entry port.**

I. Introduction

It is generally desirable to use the smallest port sizes possible in surgical robotics to reduce invasiveness. This is particularly true in the context of thoracoscopic surgery, where robots like the da Vinci are increasingly being used [1]. In such procedures, rigid instruments are inserted and manipulated by tilting them between the ribs. Many patients experience serious and chronic pain after surgery [2], [3], which has been hypothesized to come from rigid tool shafts crushing the intercostal nerves against the ribs. Thus, it is desirable to use small port sizes, and flexible instruments that can bend distally to the port, to avoid pivoting rigid tools between the ribs, in these surgeries.

Continuum robots are flexible devices that can provide tentacle-like motion [4]–[6] beyond the port, without rigid tool shafts or the need for pivoting at the entry point to the patient. The dexterity of tendon driven continuum robots makes them potentially useful in a variety of medical applications [6], [7]. These manipulators typically consist of a series of rigid disks spaced evenly along a flexible backbone, with tendons routed through holes in the periphery of each disk [8]–[11]. As tension is applied to the tendons, they apply distributed forces and moments along the manipulator [12], causing it to bend into various shapes.

These tendons apply loads to the robot's elastic backbone wherever they are constrained along the backbone and at their termination points. The larger the diameter of the robot and further away the tendons are from the backbone, the larger these loads will be for a particular tendon tension. Larger loads mean either that the robot will bend further, or that the backbone can be made stiffer, enabling larger potential forces to be applied to tissue, with less deflection of the backbone. Tendon breakage has been identified as perhaps the most significant failure point on tendon driven continuum robots [13], and it has been noted in prior studies that tendon termination points can be fragile [13]. For this reason, in this paper, we hold tension constant when comparing designs, and seek to create a manipulator that can amplify its actuation moments by increasing its diameter, after passing through a small port.

Our robot uses disks that can fold to change its diameter. The concept of folding has been explored to customize the capabilities of soft robots for various applications including grasping and locomotion (see e.g. [14], [15]). Similarly, an accordion-like folding pattern has been proposed as part of the elastic structure for a crawling tendon driven robot [16], which illustrates folding, though not diameter change. Abah et al. proposed a push-pull continuum robot with a scissor mechanism that enabled the constraint disks to change in diameter, and demonstrated in simulation how this diameter change can be used to accomplish a control task while avoiding joint limits [17]. While these previous designs demonstrate the benefits of continuum robotic manipulators which can change their size, this work demonstrates the first physical prototype of a continuum manipulator that can fit through a circular port-like constraint, then expand its diameter by over two times. This enables it to have desirable force and motion capabilities.

In this paper, we present a new tendon-driven continuum robot design which can fold along multiple planes to decrease its diameter. This enables it to fit through a port that is much smaller than its initial diameter. To do this, it uses embedded mechanical pin hinges, and includes hard-stops which prevent folding past the desired 90 degree range (Fig. 1). We show that existing mechanics-based models formulated for rigid disks still apply to our folding manipulator. We then compare to a traditional non-folding design that fits through the same port size. We show that at equivalent tendon tension, our new manipulator provides a larger workspace and greater force application capability.

* Both authors contributed equally to this work.

[1]Mariana E. Smith, Daniel S. Esser, Margaret Rox, and Robert J. Webster III are with the Department of Mechanical Engineering, Vanderbilt University, Nashville, TN, 37203. (email: Robert.Webster@Vanderbilt.edu)

[2]Alan Kuntz is with the Robotics Center and the Kahlert School of Computing at the University of Utah, Salt Lake City, UT 84112, USA.

This material is based upon work supported in part by the National Science Foundation under grant numbers 2133027 and 1935278 and the National Institutes of Health under NIBIB training grant T32EB021937. Any opinions, findings, and conclusions or recommendations expressed in this material are those of the authors and do not necessarily reflect the views of the NSF or NIH. This work is also supported in part by the SyBBURE Searle Undergraduate Research Program at Vanderbilt University.

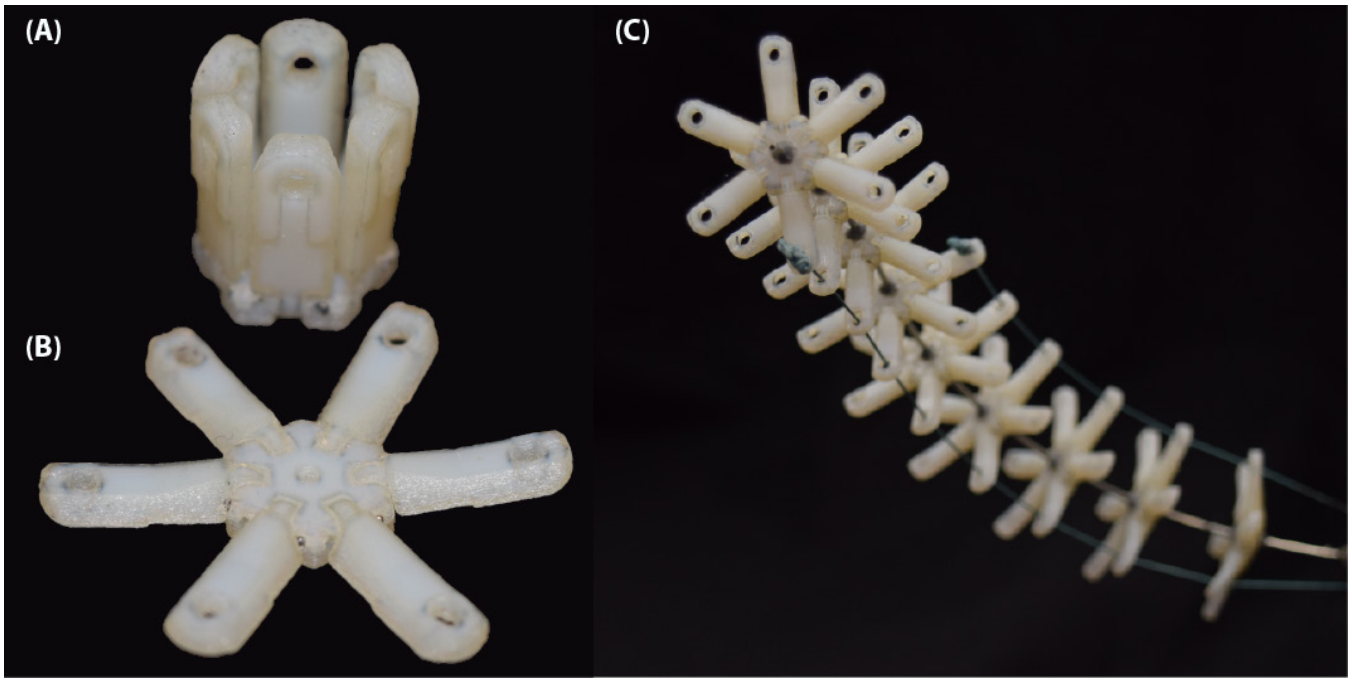

Fig. 1: (A) A folding disk shown folded and (B) open. (C) The proposed tendon driven continuum manipulator with folding disks.

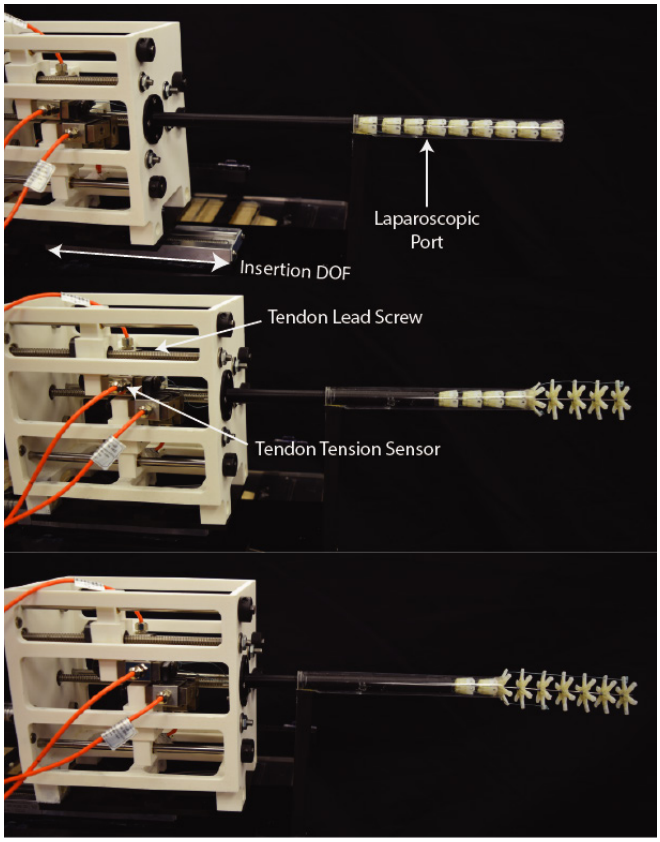

Fig. 2: Robotic system with our folding tendon manipulator at various stages of deployment through a laparoscopic port.

II. Robot Design

Our diameter-changing robot consists of a central hollow elastic backbone with support "disks", each consisting of a hub with 6 arms. The arms and central hub were printed on a Stratasys J35 polyjet printer from ABS-like resin (Stratasys: RGD-531/515), and assembled with 0.72 mm diameter steel pins. The arms fold forward so they can be deployed past the port, but can also be easily manually withdrawn through the port if the surgeon wishes to quickly remove the robot from the patient. To make the arms open after passing through the port, laser-cut rubber backing 0.4 mm thick was secured to the back of each disk with Loctite adhesive. The rubber is stretched in the folded configuration, causing the arms to naturally extend when port constraints no longer hold them closed. The hubs are secured to a Nitinol backbone using Loctite EA-9460 epoxy. The tendons in all prototypes are made from inextensible Rikimaru polymer fishing line. To evaluate this manipulator concept, we compared it directly to a standard non-folding tendon driven manipulator with the same parameters as our prototype (disk spacing, length, backbone, disk thickness) but with no deployable arms. The key parameters for both prototypes are given in Table I. The deployed diameter of 30 mm was chosen arbitrarily, and could be modified to suit specific applications in the future.

The full robotic system, shown in Fig. 2, consists of the manipulator itself (Nitinol backbone with disks affixed to it), a rigid port with a circular cross-section, and the actuation unit. The actuation unit has 5 Degrees of Freedom (DOF) for manipulator control. Four of the DOF are controlled by lead screws for the tensioning of up to four tendons, and one DOF is the insertion of the manipulator through the port. The tests performed in this paper only actuate one tendon.

TABLE I: Parameters of the tendon driven prototypes in this paper.

Parameter	Folding Design	Non-Folding Design
Deployed Diameter (d)	30 mm	12 mm
Folded Diameter (d)	12 mm	–
Deployed Hole Offset (r)	12.6 mm	3.15 mm
Folded Hole Offset (r)	4.5 mm	–
Disk Spacing (h)	13.5 mm	
Total Length (L)	216 mm	
Backbone OD	1.2 mm	
Backbone ID	0.88 mm	
Disk Thickness	2.5 mm	

Future actuation units could include additional tensioning DOFs for the control of additional tendons, and we note that the current manipulator design can accomodate up to 6 tendons which can be terminated at the tip or along the length of the manipulator, to enable piecewise curvature. The ends of each tendon are secured to load cells which sense the tension in the tendon. By securing the manipulator to the actuation unit and securing the port with respect to the ground, it is possible to translate the manipulator such that its disks travel through the port and then deploy to an open state. The manipulator's shape is changed by controlling tendon displacements, enabling complex 3D motion in both partially and fully extended configurations.

A. Modeling

We use a coupled Cosserat rod and string model [18] to determine the actuated shape of a continuum robot in this work. The model consists of a set of ordinary differential equations that are solved for the position p, orientation R, and internal forces and moment in the rod n and m:

$$\begin{aligned} \dot{p} &= \mathbf{R}v \\ \dot{\mathbf{R}} &= \mathbf{R}\hat{\omega} \\ \dot{n} &= -f \\ \dot{m} &= -\dot{p} \times n - l. \end{aligned} \tag{1}$$

The internal forces and moment can be related to the linear and angular rates of change of the body-fixed frame (v and ω) based on the constitutive elastic law:

$$\begin{bmatrix} v \\ \omega \end{bmatrix} = \mathbf{K}^{-1} \begin{bmatrix} \mathbf{R}^T n \\ \mathbf{R}^T m \end{bmatrix} + \begin{bmatrix} v^* \\ \omega^* \end{bmatrix}. \tag{2}$$

In the case of our tendon robot, the unactuated shape of the rod is given by $v^* = [0, 0, 1]^T$ and $\omega^* = [0, 0, 0]^T$. The tendons apply distributed forces and moments along their lengths, given by:

$$\begin{aligned} \mathbf{f_t} &= \sum_{i=1}^{n} \tau_i \mathbf{R} \frac{\hat{\mathbf{p}_i}^2}{\|\dot{\mathbf{p}_i}\|^3} \ddot{\mathbf{p}_i} \\ \mathbf{l_t} &= \sum_{i=1}^{n} \tau_i \mathbf{R} \mathbf{p_i}\hat{} \frac{\hat{\mathbf{p}_i}^2}{\|\dot{\mathbf{p}_i}\|^3} \ddot{\mathbf{p}_i} \end{aligned}, \tag{3}$$

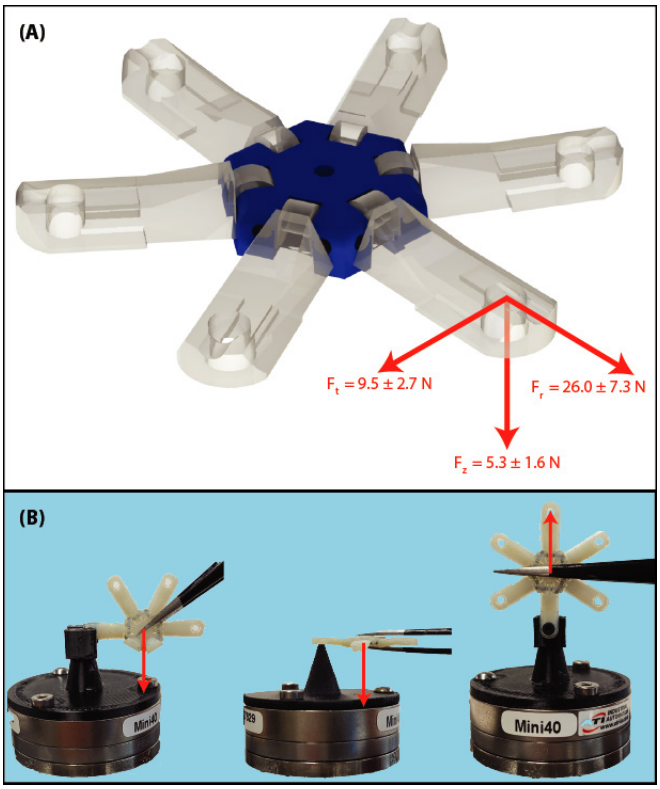

Fig. 3: (A) The three directions in which hinge breakage force was tested, and the corresponding mean force values at breakage. Arm folding occurs in the upward direction. (B) The force sensor configurations used to take breakage force measurements.

where $\mathbf{p_i}$ is the position of the i^{th} tendon relative to the center of the backbone, and τ_i is the tension applied with that tendon.

The stiffness matrix K is a diagonal matrix that relates the internal forces and moments in the rod to the deformation of the rod. The stiffness matrix for a symmetric, homogeneous rod is $K = diag(GA, GA, EA, EI_{xx}, EI_{yy}, G(I_{xx}+I_{yy})))$, where $G = \frac{E}{2(\mu+1)}$ and E are the Shear and Young's Modulus, μ is Poisson's ratio, $A = \pi(r_o^2 - r_i^2)$ is the cross-sectional area, and $I_{xx} = I_{yy} = I = \frac{\pi}{4}(r_o^4 - r_i^4)$ is the moment of area. The first three elements describe the shear stiffness in the x, y, and z directions, respectively, while the last three elements describe bending and torsional stiffness about the x, y, and z axes respectively.

Note the relationship between the bending stiffness coefficients and the geometric properties. Shear and elongation stiffness are a function of the cross-sectional area, which is proportional to radius to the second power. On the other hand, bending and torsion is a function of the second moment of area, which is proportional to radius to the fourth power. The backbone used in our manipulator is long and slender, with a small cross-section, therefore the bending stiffness is much smaller than the shear and elongation stiffness. Per equation 3, locating the tendon further away from the backbone (increasing p_i) will increase the applied moment due to the larger moment arm.

We note that there are some key modeling assumptions

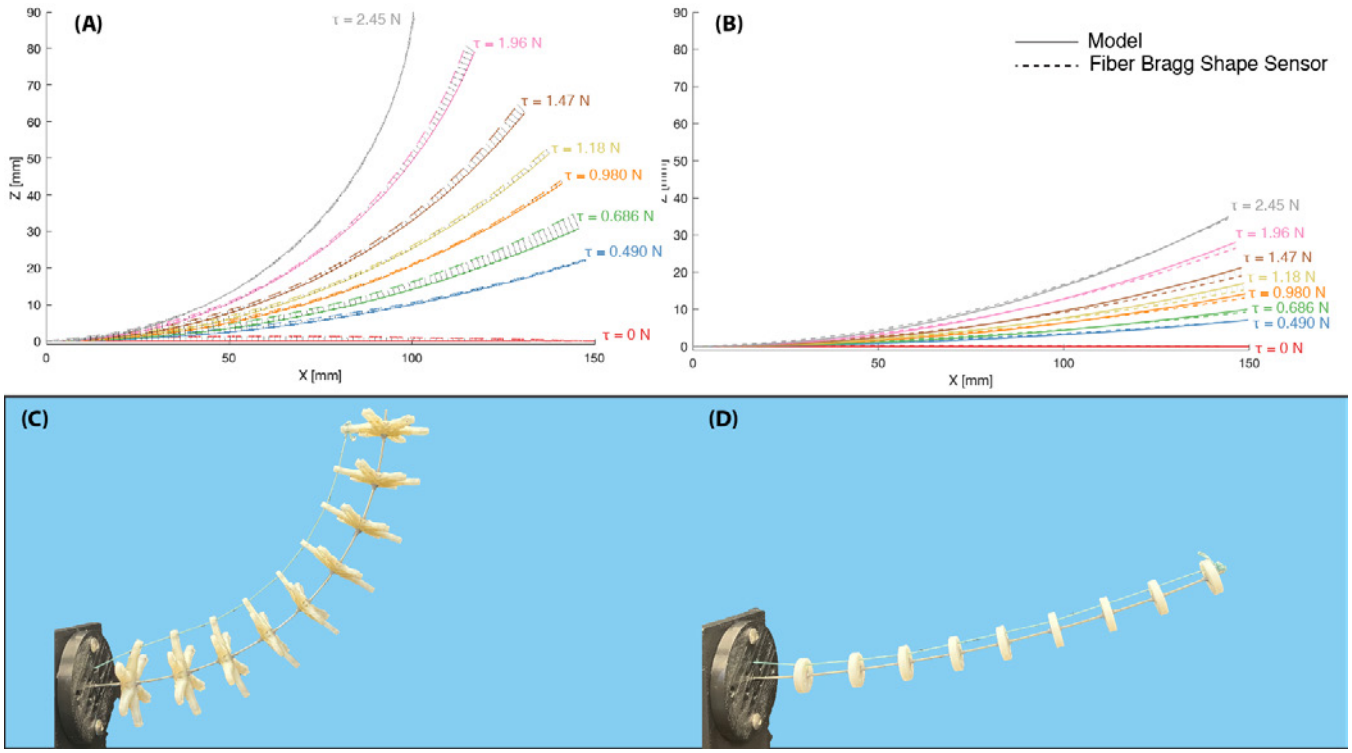

Fig. 4: The measured (dashed curves) and model (solid curves) backbone shape are compared across a range of tendon tensions for (A) a straight tendon terminating on the last disk on the folding design and (B) the nonfolding design. (C,D) Images of the prototypes with both tendons pulled at 2.45 N.

in the Cosserat rod model that must be considered when applying it to our folding prototype. Most significantly, it is assumed that the path of the tendons relative to the backbone within a cross-section is rigidly constrained, although in our proposed design the disks can fold, and there is a chance that the tendon position relative to the backbone could change if the disks open and close outside of the port. In this design, the pin hinge restricts the folding such that it takes place along a single axis. It is capable of transferring loads from the tendon to the backbone in all directions except the positive $\hat{z}$ direction, since the disks are free to fold forward. However, in the absence of friction, the tendons do not apply a significant force in this direction, so we do not observe the disks folding closed once they are deployed past the port.

III. Experiments

A. Hinge Force Testing

To test our mechanical hinge design, we determine the average force for hinge breakage in three cardinal directions. Force testing is performed using an ATI Mini-40 Force/Torque sensor. The force sensor is fixed to the benchtop and raised supports are used to enable precise force application at the tendon attachment point. The mean and standard deviation of 9 measurements taken in each principle direction are shown in Fig. 3. In each force configuration, the breakage point is located in the prototype's ABS material surrounding the pin (either in the interior disk or in the arm). In the subsequent section we demonstrate that the folding tendon robot has an acceptable range of motion with a tendon tension well below the expected failure point. Future design iterations may consider alternative fabrication techniques in order to increase the robustness of the design.

B. Model Validation and Workspace Comparison

We validate the Cosserat tendon robot model proposed in [12] on both the folding tendon robot in its deployed state, as well as the reference non-folding design, to demonstrate that the presence of the hinge joints does not significantly impact the accuracy of the model. Using a single straight-routed tendon, we apply known tensions using calibration weights hung from the tendon. We measure the full shape of the tendon robot using a fiber optic shape sensor (Pathfinder-Lab: The Shape Sensing Company) which is inserted temporarily within the inner lumen of the nitinol backbone, and affixed to the base of the manipulator using tape.

The results of the model validation are shown in Fig. 4. The average tip model prediction error for the folding robot prototype is 1.9 ± 1.4 mm. For the non-folding reference design, the tip error was 1.25 ± 0.65 mm. The results also illustrate the larger workspace of our manipulator, compared to a non-folding design actuated with the same tendon tensions.

C. Tip Force Application

We next validate the force capabilities of the folding tendon robot in its deployed state compared to the non-folding reference. As in the model validation experiment, a single straight-routed tendon was used to apply known

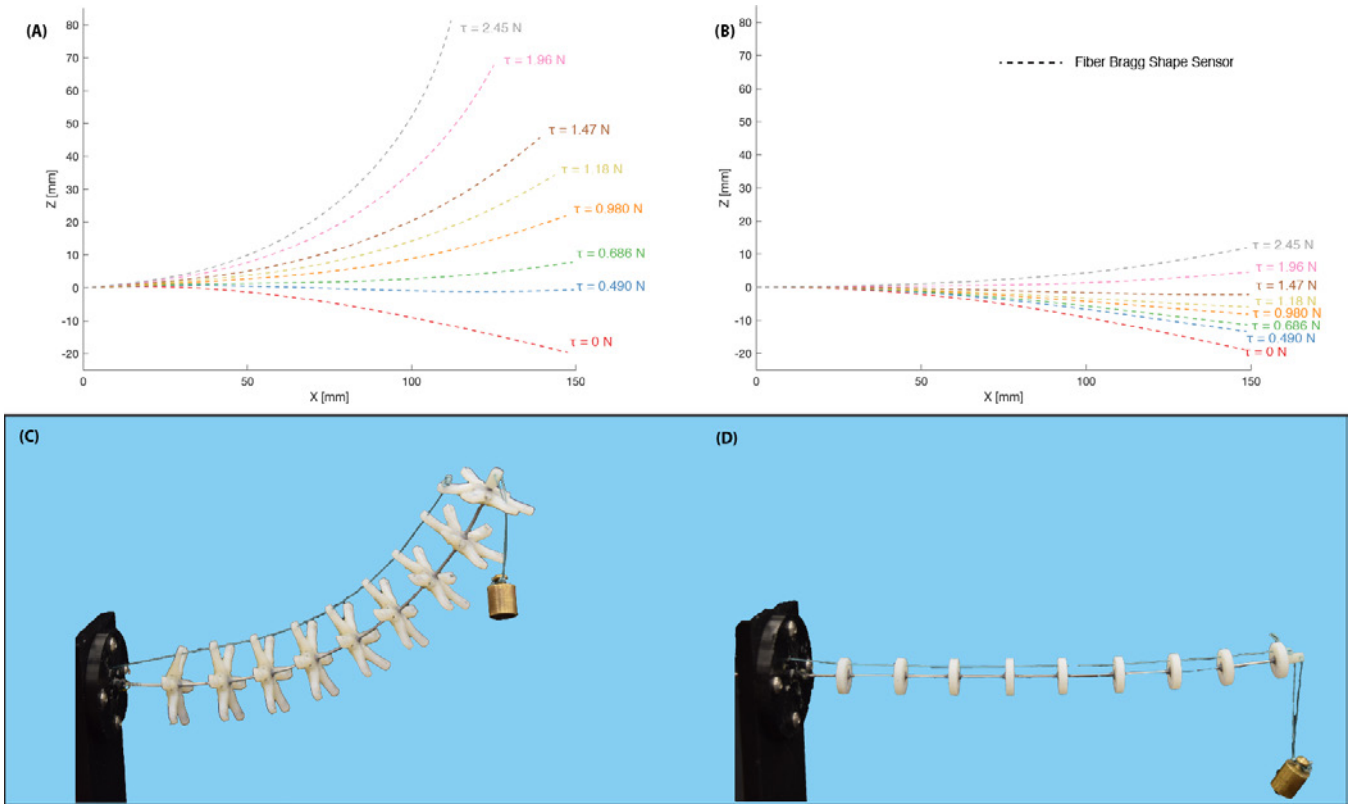

Fig. 5: Backbone shape of (A) the folding robot and (B) the nonfolding robot, with each lifting a point load, with shape measured using the fiber shape sensor, at various tendon tensions. (C,D) A single, initially straight tendon was pulled at a range of tensions with a 5g mass affixed to the tip of the manipulator.

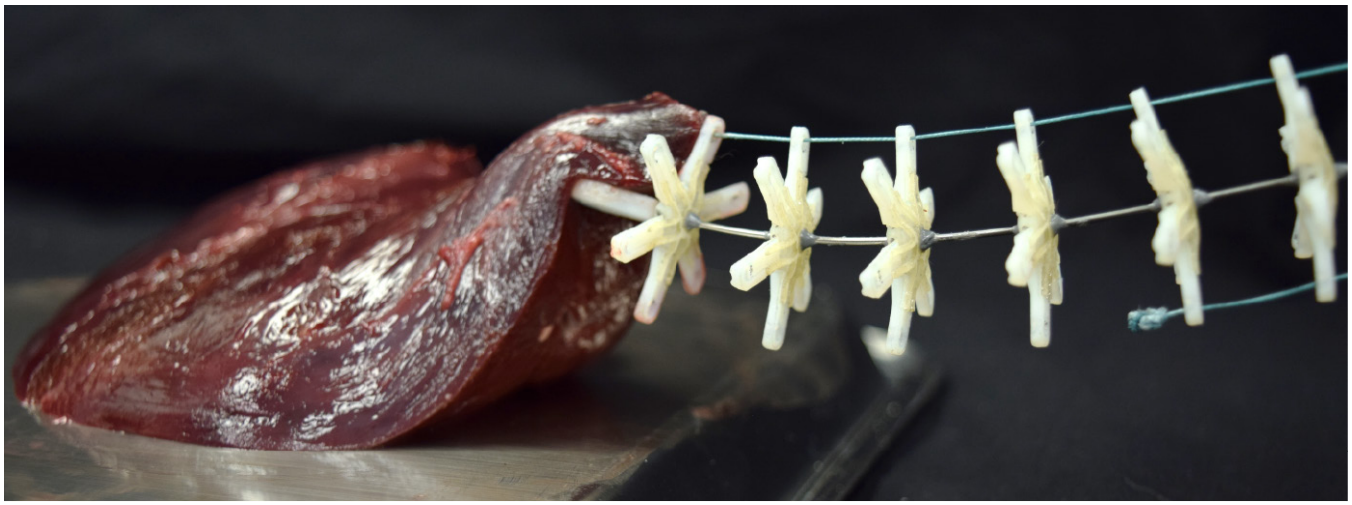

Fig. 6: The folding tendon robot retracting animal tissue.

tensions using calibration weights, and the full shape of the robot was measured with the fiber optic shape sensor. A hanging 5 gram mass was secured to the tip of the robot to mimic an external loading condition. The results of robot shape during a sweep of increasing tendon tensions with an applied tip load are shown in Fig. 5. Our deployed manipulator is capable of lifting its tip 81 mm above the straight (horizontal) configuration when under 5 grams of tip loading with 2.45 N applied to the tendon. In contrast, the non-folding design is only capable of lifting its tip up 12 mm when subject to the same loading condition and tendon tension.

D. Retracting Tissue

We envision our manipulator design as advantageous for a variety of clinical applications which require a small incision site, high dexterity, and applying force to the surgical environment. One such application is the retraction of tissue.

In Fig. 6, a stiff retractor tip is secured to the tip of the manipulator. Our robot is then used to lift a lobe of ex-vivo bovine liver, demonstrating a first proof-of-concept application for this design.

IV. Conclusion

This paper presents a novel tendon-driven continuum robot design that can change its diameter using radially folding arms. This enables the manipulator to pass through a small port, and then expand inside the body to amplify the actuation moments applied by its tendons, for a given tendon tension. When our manipulator is past the port with unfolded disks, we demonstrated that its shape can be predicted well by existing mechanics-based models. Furthermore, we demonstrated that at the same tendon tension, it has a superior range of motion to a non-folding design that can fit through the same port size. We also showed that with the same tendon tensions, it can lift the same load higher. A current limitation of our prototyping methods is the strength of the pin hinge joint, although we believe that this can be addressed with design and fabrication improvements that mechanically reinforce this area by adding thickness or changing materials. Having a large number of equally spaced tendon supports (6 in our prototype) is desirable because it enables one to thread tendons through many possible non-linear paths along the backbone. However use of a smaller number would enable the design to be miniaturized or the pin joints strengthened by increasing wall thickness around the hinges. While future improvements are possible, the design in this paper fulfills its intended purpose of demonstrating the feasibility of fitting a tentacle-like robot through a port that is less than half the size of its expanded diameter. Both the small port and the elimination of a rigid tool shaft pivoting at the body wall may be beneficial in the future to reduce invasiveness and potential complications. This is particularly true in the minimally invasive lung surgery application that motivated this work, where a design such as ours may reduce post-operative pain associated with nerve damage.

References

[1] F. Al-Mufarrej, M. Margolis, B. Tempesta, E. Strother, F. Najam, and F. Gharagozloo, "From jacobeaus to the da vinci: thoracoscopic applications of the robot," *Surgical Laparoscopy, Endoscopy & Percutaneous Techniques*, vol. 20, pp. 1–9, 2010.

[2] T. Homma, Y. Doki, Y. Yamamoto, T. Ojima, Y. Shimada, N. Kitamura, and N. Yoshimura, "Risk factors of neuropathic pain after thoracic surgery," *Journal of Thoracic Disease*, vol. 10, pp. 2898–2907, 2018.

[3] M. Bendixen, O. D. Jørgensen, C. Kronborg, C. Andersen, and P. B. Licht, "Postoperative pain and quality of life after lobectomy via video-assisted thoracoscopic surgery or anterolateral thoracotomy for early stage lung cancer: a randomised controlled trial," *The Lancet. Oncology*, vol. 17, no. 6, pp. 836–844, 2016.

[4] I. D. Walker, "Continuous backbone continuum robot manipulators," *ISRN Robotics*, vol. 2013, 2013.

[5] R. J. Webster and B. A. Jones, "Design and kinematic modeling of constant curvature continuum robots: A review," *The International Journal of Robotics Research*, vol. 29, p. 1661–1683, 2010.

[6] J. Burgner-Kahrs, D. C. Rucker, and H. Choset, "Continuum robots for medical applications: A survey," *IEEE Transactions on Robotics*, vol. 31, no. 6, p. 1261–1280, 2015.

[7] T. D. Veiga, J. H. Chandler, P. Lloyd, G. Pittiglio, N. J. Wilkinson, A. K. Hoshiar, R. A. Harris, and P. Valdastri, "Challenges of continuum robots in clinical context: a review," *Progress in Biomedical Engineering*, vol. 2, p. 032003, 2020.

[8] M. Calisti, A. Arienti, F. Renda, G. Levy, B. Hochner, B. Mazzolai, P. Dario, and C. Laschi, "Design and development of a soft robot with crawling and grasping capabilities," *IEEE International Conference on Robotics and Automation*, p. 4950–4955, 2012.

[9] T. Ranzani, G. Gerboni, M. Cianchetti, and A. Menciassi, "A bioinspired soft manipulator for minimally invasive surgery," *Bioinspiration & Biomimetics*, vol. 10, pp. 035 008–035 008, 2015.

[10] H. Wang, W. Chen, X. Yu, T. Deng, X. Wang, and R. Pfeifer, "Visual servo control of cable-driven soft robotic manipulator," *2013 IEEE/RSJ International Conference on Intelligent Robots and Systems*, pp. 57–62, 2013.

[11] E. Amanov, T. D. Nguyen, and J. Burgner-Kahrs, "Tendon-driven continuum robots with extensible sections—a model-based evaluation of path-following motions," *International Journal of Robotics Research*, vol. 40, 2021.

[12] D. C. Rucker and R. J. Webster III, "Statics and dynamics of continuum robots with general tendon routing and external loading," *IEEE Transactions on Robotics*, vol. 27, no. 6, 2011.

[13] U. Jeong, K. Kim, S. H. Kim, H. Choi, B. D. Youn, and K. J. Cho, "Reliability analysis of a tendon-driven actuation for soft robots," *International Journal of Robotics Research*, vol. 40, no. 1, 2021.

[14] E. Diller and M. Sitti, "Three-dimensional programmable assembly by untethered magnetic robotic micro-grippers," *Advanced Functional Materials*, vol. 24, pp. 4397–4404, 2014.

[15] Y. Sun, D. Li, M. Wu, Y. Yang, J. Su, T. Wong, K. Xu, Y. Li, L. Li, X. Yu, and J. Yu, "Origami-inspired folding assembly of dielectric elastomers for programmable soft robots," *Microsystems & Nanoengineering*, vol. 8, pp. 37–37, 2022.

[16] H. Banerjee, N. Pusalkar, and H. Ren, "Single-motor controlled tendon-driven peristaltic soft origami robot," *Journal of Mechanisms and Robotics*, vol. 10, 2018.

[17] C. Abah, A. L. Orekhov, and N. Simaan, "Design considerations and redundancy resolution for variable geometry continuum robots," *IEEE International Conference on Robotics and Automation*, pp. 767–774, 2018.

[18] D. C. Rucker, B. A. Jones, and R. J. Webster III, "A geometrically exact model for externally loaded concentric-tube continuum robots," *IEEE Transactions on Robotics*, vol. 26, no. 5, p. 769–780, 2010.